

RoboMemory: A Brain-inspired Multi-memory Agentic Framework for Interactive Environmental Learning in Physical Embodied Systems

Mingcong Lei^{1,3,*}, Honghao Cai^{1,*}, Zezhou Cui^{1,3}, Liangchen Tan⁴, Junkun Hong¹
 Gehan Hu^{1,3}, Shuangyu Zhu^{1,6}, Yimou Wu³, Shaohan Jiang^{1,3}, Ge Wang^{1,3}, Yuyuan Yang³
 Junyuan Tan¹, Zhenglin Wan⁵, Zhen Li^{1,2}, Shuguang Cui^{1,2}, Yiming Zhao^{1,7,8}, Yatong Han^{1,8}
¹ FNii-Shenzhen ² SSE ³ The Chinese University of Hong Kong, Shenzhen
⁴ The University of Hong Kong ⁵ Nanyang Technological University
⁶ Harbin Institute of Technology, Shenzhen ⁷ Harbin Engineering University ⁸ Infused Synapse AI
 yiming.zhao@hrbeu.edu.cn hanyatong@cuhk.edu.cn
 Project website: <https://sp4595.github.io/robomemory/>

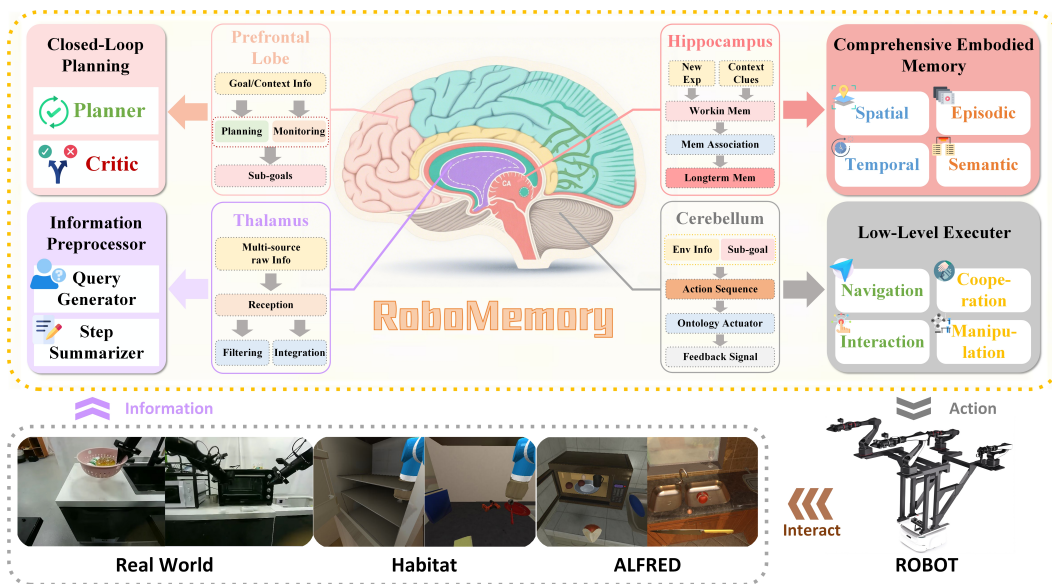


Figure 1: RoboMemory adopts a brain-inspired architecture that maps neural components to agent modules, enabling long-term planning and interactive learning across diverse environments (real-world, Habitat, ALFRED) and robotic hardware.

Abstract

Embodied agents face persistent challenges in real-world environments, including partial observability, limited spatial reasoning, and high-latency multi-memory integration. We present RoboMemory, a brain-inspired framework that unifies Spatial, Temporal, Episodic, and Semantic memory under a parallelized architecture for efficient long-horizon planning and interactive environmental learning. A dynamic spatial knowledge graph (KG) ensures scalable and consistent memory updates, while a closed-loop planner with a critic module supports adaptive decision-making in dynamic settings. Experiments on EmbodiedBench show

*Equal contribution

that RoboMemory, built on Qwen2.5-VL-72B-Ins, improves average success rates by 25% over its baseline and exceeds the closed-source state-of-the-art (SOTA) Gemini-1.5-Pro by 3%. Real-world trials further confirm its capacity for cumulative learning, with performance improving across repeated tasks. These results highlight RoboMemory as a scalable foundation for memory-augmented embodied intelligence, bridging the gap between cognitive neuroscience and robotic autonomy.

1 Introduction

Recent advances in Vision-Language Models (VLMs) [21, 3] have enabled their growing use in embodied tasks [30, 20]. VLM-based embodied agents can process multimodal inputs and generate high-level textual commands (e.g., “Pick up the cup”), which require translation via tool APIs to become executable robot actions. In contrast, Vision-Language-Action models (VLAs) [22, 5, 4, 11] produce low-level control signals directly but generally rely only on the latest observation. This limits their ability to perform long-horizon, multi-step tasks that require reasoning over task history. In summary, VLA models enable direct robot control but lack high-level planning capabilities, and VLM-based embodied agents support strategic planning but struggle with direct motor control. This highlights a key gap inherent in two distinct technical approaches to embodied intelligence.

To bridge this gap, recent work [43, 31, 34] proposes a “VLM planner + VLA executor” paradigm. Here, VLM-based embodied agents serve as high-level planners that decompose complex tasks (e.g., “make a coffee”) into executable sub-instructions (e.g., “grasp the cup”) that VLAs can complete. Although this paradigm improves performance on multi-step tasks, prior work suffers from two key limitations in real-world settings. First, real-world tasks (e.g., kitchen operations) require navigating across multiple locations to gather objects and tools, but the environment remains only partially observable at any time due to robots’ limited field of view and dynamic occlusions. This necessitates a planner with robust spatial awareness and long-term memory to maintain a consistent spatial awareness across viewpoints. However, most VLM-based agents rely on chat-style context windows (e.g., logging instruction – feedback pairs [42]), which lack mechanisms for maintaining an overview of the environment’s spatial layout. Consequently, agents cannot reliably track object locations or recognize previously visited states. Second, pretrained VLMs are rarely trained on embodied planning trajectories, especially long-horizon, spatially grounded ones. So VLM-based agents often struggle to generalize to real-world settings [40]. To overcome these challenges, VLM-based planners must support interactive environmental learning — the ability to acquire, integrate, and retrieve spatial, episodic, and semantic knowledge during task execution, thereby enabling adaptation through experience.

To support long-horizon planning and interactive learning in real-world settings, agents require a comprehensive memory system with multiple specialized modules. Recent frameworks [35, 17, 38, 1, 14, 46, 8] have integrated Retrieval-Augmented Generation (RAG)-based memory to enhance planning and interactive environmental learning [16], but most are designed for simulated environments. A key limitation for real-world deployment is the absence of spatial memory, which is critical for building spatial awareness and providing context for planning. Additionally, existing multi-module memory systems often incur significant inference latency.

To overcome these limitations, especially the need for memory that is efficient, spatially grounded, and persistent in dynamic environments, we return to the essence of intelligence — how does the human brain plan, remember, and learn in dynamic environments? Inspired by cognitive neuroscience, we have designed RoboMemory, a parallel multi-memory architecture that simulates key functional regions of the brain. RoboMemory features a hierarchical and parallelized architecture enabling long-term planning and continuous adaptation. Drawing inspiration from cognitive neuroscience [27], RoboMemory comprises four core components (Figure 1): (1) Information Preprocessor (thalamus-inspired) for multimodal sensory integration. (2) Comprehensive Embodied Memory System (hippocampus-inspired), which organizes experiential and spatial knowledge through a three-tier structure (long-term, short-term, and sensory memory). Within this tiered system, four memory modules: Spatial, Temporal, Episodic, and Semantic operate under a unified, parallel-update paradigm to enable coherent knowledge integration while minimizing latency. (3) Closed-Loop Planning Module (prefrontal cortex-inspired) for high-level action sequencing. These three modules provide a high-level planner with comprehensive sensory and memorization ability.

(4) Low-level Executor (cerebellum-inspired), consisting of a VLA-based operation model and a SLAM-based navigation model. The Low-level Executor directly controls the robot with low-level control signals to navigate and operate in the real-world environment.

To verify whether RoboMemory truly addresses the problems of long-horizon planning and interactive learning, we evaluate RoboMemory on EmbodiedBench, a long-horizon planning benchmark [40]. Using Qwen2.5-VL-72B as the base model, RoboMemory improves average success rates by 25% over its base model and 3% over the closed-source state-of-the-art model, Gemini-1.5-Pro. In real-world trials, RoboMemory executed diverse tasks twice consecutively: once for environmental familiarization (learning phase) and once for memory-augmented execution (testing phase) without resetting memory. The observed performance improvement validates RoboMemory’s capacity for interactive environmental learning. We further conduct ablation studies and error analysis to quantify component contributions and identify remaining limitations. We summarize our contribution as follows:

- We propose a brain-inspired unified embodied memory system, integrating four concurrently updated modules (Spatial, Temporal, Episodic, Semantic) into a single framework. It enables efficient, comprehensive memory operations and coherent knowledge integration, which are critical for interactive environmental learning in real-world embodied scenarios.
- We design a retrieval-based incremental update algorithm for real-time evolution of Spatial Knowledge Graphs (KGs). By retrieving relevant subgraphs, detecting local inconsistencies, and merging new observations, it ensures efficient, consistent KG maintenance and addresses the scalability bottleneck of previous KG-based methods in embodied settings.
- RoboMemory supports interactive environmental learning for real-world physical robots: it enables sequential diverse tasks without memory reset, with experience accumulation driving steady performance improvements, demonstrating practical long-term autonomous learning in physical scenarios.

2 RoboMemory

RoboMemory is a hierarchical embodied agent system that equips robots with three core memory capabilities: historical interaction logs, dynamically updated spatial layouts, and accumulated task knowledge. As illustrated in Figure 2, each iteration, RoboMemory follows a process of “Perception – Memory – Retrieval – Planning – Execution” process, ensuring that the agent continuously calibrates its memory and behavior in dynamic environments.

First, the information preprocessor converts multimodal sensor inputs into a textual summary of the current scene, which serves as the primary input to the Comprehensive Embodied Memory. Next, the Comprehensive Embodied Memory updates its internal representations, including action histories, object locations, and experiential knowledge. After information is updated, the memory system retrieves contextually relevant entries to inform the Closed-Loop Planning Module. Then, leveraging this contextual memory, the Closed-Loop Planning Module generates high-level, text-based action instructions. Finally, these commands are dispatched to low-level executors, who will directly control the robot and complete the instructions.

2.1 Information Preprocessor

At each time step i , RoboMemory receives a visual observation \mathcal{O}_i : an RGB frame (in simulation) or a short video clip (on physical robots), representing the agent’s observations.

Since raw visual data is unsuitable for direct use in memory construct and retrieval, RoboMemory first employs an information preprocessor to convert multimodal observations into textual representations, thereby providing a semantic interface for subsequent memory and planning modules. The information preprocessor executes two Vision-Language Models (VLMs) in parallel: (1) *Step summarizer* \mathcal{S} : Transforms \mathcal{O}_i into a concise textual description s_i of the just-executed action. The string s_i is stored in the system’s working memory. (2) *Query generator* \mathcal{Q} : Derives a query q_i from the same observation \mathcal{O}_i , which is used to probe long-term memory for relevant episodes.

Together, \mathcal{S} and \mathcal{Q} provide a swift, text-based interface between raw sensory data and provide basic information in each iteration for RoboMemory’s Comprehensive Embodied Memory System.

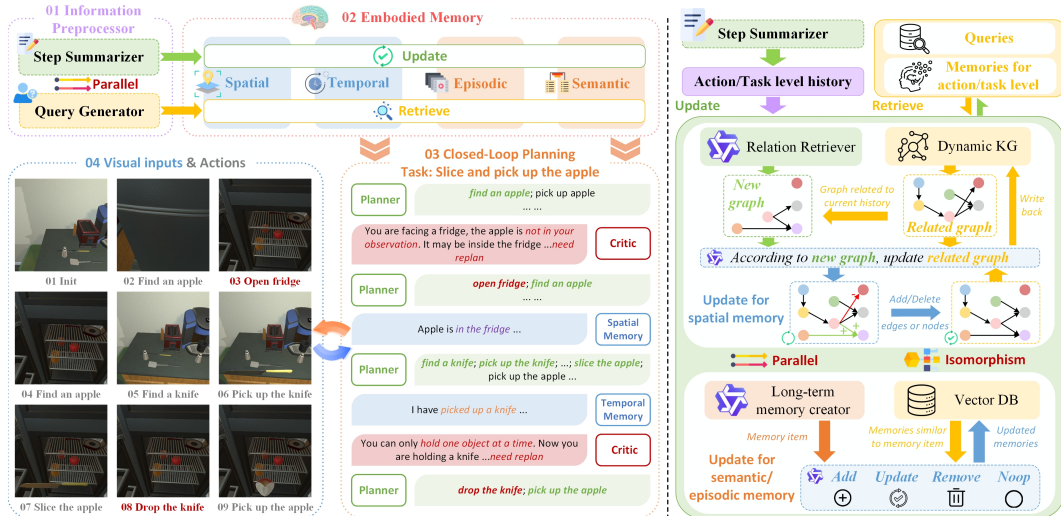


Figure 2: RoboMemory architecture. (a) Left: Parallel Step Summarizer and Query Generator generate updates/queries for Comprehensive Embodied Memory. These memories enable Closed-Loop Planning for tasks like “slice and pick up the apple”—the Planner generates plans, while the Critic and memories adjust decisions via feedback from visual inputs/results. (b) Right: Spatial memory maintains a relevance/similarity-updated KG, and Semantic/Episodic memory manages a Vector DB with analogous logic. Besides, Temporal memory is implemented as a linear FIFO buffer that stores step-wise summaries generated by the Step Summarizer.

2.2 Comprehensive Embodied Memory System

We present a high-level memory system designed to enhance embodied agents’ long-horizon planning and enable interactive learning in dynamic, partially observable environments. Built on RAG and KG technologies [18], the system comprises Spatial-Temporal Memory and Long-Term Memory. Spatial-Temporal Memory continuously encodes object relationships and environmental layouts, as well as detailed task execution traces. These records inform Long-Term Memory, which goes through spatial-temporal information collected in each task, capturing what strategies succeeded or failed and relevant environmental facts (Figure 2).

The Comprehensive Embodied Memory module receives summarized sensory information from the information preprocessor to update both memory components in real time. Critically, all updates and retrievals are performed in parallel, ensuring efficient operation even under multiple active memory modules.

2.2.1 Spatial-Temporal Memory System

Due to the dynamic and partially observable nature of real embodied environments, completing long-term tasks requires dynamically maintaining a spatial-temporal memory system. The system records the agent’s interaction history with the environment and maintains a continuously updated spatial model of the current surroundings. To achieve these two purposes, we design spatial memory and temporal memory. The combination of spatial and temporal memory provides the embodied agent with comprehensive contextual awareness, supporting effective planning and interactive environmental learning in real-world settings.

Temporal Memory. Interactions between the robot and the environment must be recorded. For such temporally sequential memory, a simple structure suffices: a sequential buffer with automatic summarization triggered upon reaching capacity. The buffer tracks the high-level actions from the Embodied Agent, how the low-level executor actually controls the robot, and the environmental feedback received. In a specific design, temporal memory can store up to N interaction summaries, each generated by an information preprocessor. When the buffer is full, rather than discarding old entries outright, we compress the oldest N steps into a single summarized entry using a VLM, which is then reinserted at the front of the buffer, ensuring continuous context retention without unbounded growth.

Spatial Memory. Current spatial memory approaches often rely on RGB-D cameras to reconstruct 3D point clouds [44, 7]. However, such representations are overly detailed for high-level planning in embodied agents — precise geometric relationships (e.g., exact distances between objects) are unnecessary. Moreover, point clouds are difficult to update efficiently in dynamic scenes.

To address these problems, we advocate for an abstracted spatial memory that captures object-level entities and their spatial relationships. Inspired by [18], we represent this memory as a KG: objects become vertices, and spatial relations are encoded as edges. The KG focuses on high-level spatial relations (e.g., “cup on table”, “key left of drawer”). Unlike geometric representations that encode precise coordinates, which are often irrelevant for high-level planning, our KG focuses on semantically meaningful, task-relevant relations. This abstraction enhances the agent’s spatial reasoning capability in dynamic environments. In our memory system, spatial memory is a dynamic KG storing high-level spatial knowledge. To overcome the limited spatial reasoning of embodied agents in dynamic environments, we use a KG.

We introduce a retrieval-driven, incremental KG update algorithm that maintains a locally modifiable, globally consistent, and dynamically adaptive spatial memory. As illustrated in the right panel of Figure 2, the update process proceeds in four steps: (1) retrieves the most relevant sub-KG around new observations. (2) Injects new relations from the current observation by a VLM-based Relation Retriever. (3) Detects and resolves conflicts between newly extracted relations and existing ones (e.g., “cup on table” vs. “cup in drawer”) using a VLM-based resolver, which decides whether to add, delete, or modify edges. (4) Merges back and prunes isolated vertices. Moreover, our retrieval-based incremental update algorithm comes with provable efficiency guarantees: for a KG with n vertices and maximum degree D , the number of vertices processed per update is bounded by $O(D^K)$, where K is the retrieval hop distance (see Appendix C.3 for formal analysis). Further architectural and implementation details are provided in Appendix C.1.

2.2.2 Interactive Environmental Learning System

Although episodic memory can record “what happened,” it cannot directly answer “why it succeeded/failed” or “what should be done next time.” Drawing on cognitive psychology’s classification of human long-term memory, we divide our system into episodic and semantic memory: the former records agent-environment interaction histories, while the latter extracts experiential insights to support long-term task reasoning. This update process mirrors human daily experience consolidation during sleep [25].

Episodic Memory: It captures task-level interactions, accounting for temporal interdependencies between sequential tasks in the same environment. The agent must memorize what it has done before to complete future tasks. Moreover, task-level interactions can be a reference that may help the agent improve its plan in the future.

Semantic Memory: It accumulates step-by-step action usage experiences (based on invoked actions and outcomes) to inform action arrangement. Post-task, it summarizes temporal memory, distilling successes from completed tasks and identifying failure causes/improvement strategies from unsuccessful ones, thus enabling both action-level and task-level learning across both task and action levels.

In implementation, both episodic and semantic memory share the same RAG framework consisting of an extractor, updater, and RAG storage (each entry is a memory entity). Post-task, the Extractor summarizes the task’s Spatial-Temporal Memory into a new memory entity. The RAG then retrieves similar existing entities (old information) from the RAG. Then, the Updater deletes, adds, or updates old memory entities according to new information. After that, we write the updated memory entities back to the RAG. Because we only update memory entities similar to new information, efficiency is ensured by restricting updates to old memory entities relevant to the new entity instead of all memory entities stored in the RAG.

2.3 Closed-Loop Planning Module for Dynamic Environment

The Closed-Loop Planning Module integrates information about the current task provided by the Spatial-Temporal Memory, Semantic and Episodic information recorded in long-term memory, and current observations to perform action planning. Each action is planned and passed on to the low-level executor for execution.

To enable closed-loop control in embodied environments, the Closed-Loop Planning Module adopts the Planner-Critic mechanism [23], which consists of the planner and the critic module. For each planning step, the planner generates a long-term plan consisting of multiple steps. However, due to the dynamics of embodied environments, the action sequence in the long-term plan may become outdated during the execution of the plan. Thus, before executing each step, we use the Critic model to evaluate whether the proposed action in this step remains appropriate under the latest environment. If not, the planner will re-plan based on the latest information. The demonstration of this process is shown in Figure 2.

However, our experiments reveal that the original Planner-Critic mechanism may suffer from infinite loops. In the original mechanism, the first step of the action sequence output by the Planner is evaluated by the Critic before execution, which can lead to an infinite loop: if the Critic always demands replanning, no action will ever be executed. To address this, we modified the Planner-Critic mechanism so that the first step is not evaluated by the Critic. This ensures that even if the Critic persistently demands replanning, the RoboMemory will still execute actions.

2.4 Low-level Executor

The RoboMemory framework is a two-layer hierarchical agent framework. This design enables RoboMemory to accomplish longer-term tasks in the real world. The upper layer is responsible only for high-level planning, while the Low-level Executor carries out the actions planned by the upper layer in the real environment.

We employ a LoRA-finetuned VLA model, π_0 [19, 5], to generate manipulation actions, and a SLAM-based navigation model for locomotion. The low-level executor then translates high-level actions planned by RoboMemory into concrete arm and chassis movements in the real world.

Table 1: Comparison of Success Rates (SR) and Goal Condition Success Rates (GC) across difficulty levels between RoboMemory and baseline methods on EB-ALFRED.

Method	Type	Avg.		Base		Long	
		SR	GC	SR	GC	SR	GC
Single VLM-Agents							
GPT-4o	Closed-source	59.0 %	68.3 %	64.0 %	74.0 %	54.0 %	62.5 %
GPT-4o-mini		17.0 %	32.4 %	34.0 %	47.8 %	0.0 %	17.0 %
Claude-3.5-Sonnet		62.0 %	63.3 %	72.0 %	72.0 %	52.0 %	54.5 %
Gemini-1.5-Pro		64.0 %	69.7 %	70.0 %	74.3 %	58.0 %	65.0 %
Gemini-2.0-flash		60.0 %	63.9 %	62.0 %	65.7 %	58.0 %	62.0 %
Llama-3.2-90B-Vision-Ins		Open-source	27.0 %	33.9 %	38.0 %	43.7 %	16.0 %
InternVL2.5-78B	40.0 %		45.7 %	38.0 %	42.3 %	42.0 %	49.0 %
InternVL3-78B	37.0%		-	38.0%	-	36.0%	-
InternVL2.5-38B	31.0%		36.9%	36.0%	37.3%	26.0%	36.5%
Qwen2.5-VL-72B-Ins	42.0 %		-	50.0 %	-	34.0 %	-
VLM-Agent Frameworks							
Voyager (Qwen2.5-VL-72B-Ins)	Baselines	44.0%	63.7%	56.0%	73.2%	32.0%	54.2%
Reflexion (Qwen2.5-VL-72B-Ins)		29.0%	43.2%	48.0%	54.0%	10.0%	33.0%
Cradle (Qwen2.5-VL-72B-Ins)		43.0%	54.6%	54.0%	67.9%	32.0%	41.0%
RoboMemory (Qwen2.5-VL-72B-Ins)	Ours	67.0 %	78.4 %	68.0 %	75.5 %	66.0 %	81.3 %

3 Experiments

3.1 Benchmarks

To evaluate the task planning ability of RoboMemory, we select a subset of the EB-ALFRED benchmark from EmbodiedBench[40]. We selected the Base and Long subsets because they aim to test the agent’s planning ability. The Base and Long subset comprises 100 tasks for complex embodied tasks. The EB-ALFRED environment provides a visually-grounded operational setting that closely mimics real-world conditions (see Appendix D for environment details), enabling direct comparison with established baselines.

Additionally, we have also evaluated RoboMemory’s capabilities on the EB-Habitat benchmark [40]. For detailed results, please refer to Appendix B.

Moreover, we set up an environment to test the interactive environmental learning ability of RoboMemory in the real world.

3.2 Settings & Baselines

To facilitate comparisons, we consider two types of baselines. First, we choose the advanced closed-source and open-source VLMs as a single agent. We compare their performance with RoboMemory. For closed source VLMs, we choose GPT-4o and GPT-4o-mini [28, 21], Claude3.5-Sonnet [2], Gemini-1.5-Pro and Gemini-2.0-flash [36, 13]. For open source VLMs, we choose Llama-3.2-90B-Vision-Ins [26], InternVL-2.5-78B/28B [10], InternVL-3-72B [48], and Qwen2.5-VL-72B-Ins [3]. Secondly, we choose three agent frameworks: (1) Reflexion [32], which introduces a simple long-term memory and a self-reflection module. Reflexion uses the self-reflection module to summarize experiences as long-term memory, thereby enhancing the model’s capabilities. (2) Voyager [38], which utilizes a skill library as its procedural memory, is a widely used baseline for embodied agent planning. (3) Cradle [35], which proposes a general agent framework with episodic and procedural memory and gains good performances at various multi-model agent tasks.

In our experiments, each agent framework is tested using Qwen2.5-VL-72b-Ins [37]. The Qwen2.5-VL-72b-Ins represents a high-performing open-source alternative. Notably, the Qwen2.5-VL-72b-Ins demonstrates performance comparable to advanced closed-source VLMs in several benchmark tasks [39]. We use the Qwen3-Embedding model [45] to create embedding vectors for RAGs in RoboMemory. For the Low-level Executor, since EB-ALFRED provides high-level action APIs, we use the low-level executor provided by EmbodiedBench instead of the VLA-based method.

We define two evaluation metrics to assess the performance: (1) Success Rate (SR), which is the ratio of completed tasks to the total number of tasks in each difficulty level. This metric reflects the agent’s ability to complete tasks across randomly generated scenarios. (2) Goal Condition Success Rate (GC), which is the ratio of intermediate conditions achieved to the maximum possible score in each scenario. An GC of 100% indicates that the task is completed in the given scenario. These two metrics can be computed as:

$$SR = \mathbb{E}_{x \in \mathcal{X}} [\mathbb{1}_{SCN_x = GCN_x}] \tag{1}$$

$$GC = \mathbb{E}_{x \in \mathcal{X}} \left[\frac{SCN_x}{GCN_x} \right] \tag{2}$$

Where \mathcal{X} denotes the test subset, and x represents a test task. The success condition number (SCN_x) refers to the number of conditions the agent has accomplished, while the global condition number (GCN_x) indicates the total number of conditions required for task completion. The task is considered successful if $SCN_x = GCN_x$.

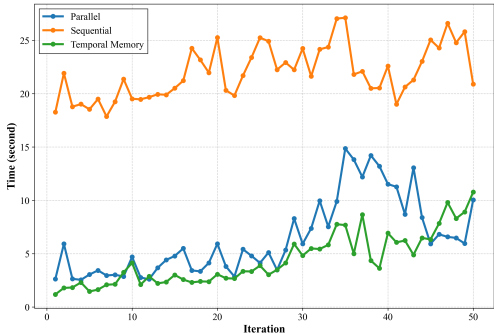


Figure 3: Efficiency improvement of Comprehensive Embodied Memory System

Table 2: Ablation Study on RoboMemory’s Success Rate (SR)

Method	Avg.	Base	Long
RoboMemory	67%	68%	66%
- w/o critic	55%	60%	50%
- w/o spatial memory	47%	52%	42%
- w/o long-term memory	57%	66%	48%
- w/o episodic memory	62%	68%	56%
- w/o semantic memory	58%	66%	50%

3.3 Main results

As shown in Table 1, our model achieves significant improvements over both single VLM agents and Agent frameworks on the EB-ALFRED. Compared to the SOTA Single VLM-Agent model, Gemini1.5-Pro, RoboMemory with Qwen2.5-VL-72B-Ins backbone improves the average SR by 3% and GC by 8.7%. This demonstrates RoboMemory’s superiority over single VLM-Agents, proving that an Agent framework with open-source models can outperform closed-source SOTA models. Furthermore, when tested against other VLM-Agent frameworks, RoboMemory also shows substantial gains. This is because, unlike other frameworks, RoboMemory’s brain-like memory system provides embodied models with more accurate and persistent contextual information. Additionally, the Planner-Critic mechanism provides a closed-loop planning ability, which helps the RoboMemory gain better performance in long-term tasks. Because the RoboMemory can detect and try to overcome possible failures. And it is more robust when encountering unexpected situations.

3.4 Efficiency Analysis

To evaluate the efficiency of the Comprehensive Embodied Memory module, we tasked RoboMemory with executing 10 long-horizon tasks, each comprising approximately 50 steps. We exclusively measured the wall-clock time consumed by memory update and retrieval operations. We analyzed the scaling behavior of memory update latency across three distinct configurations: (1) fully parallel update and retrieval across all memory modules; (2) sequential update of each memory module without parallelism; and (3) update of only the most fundamental memory component: the Temporal Memory. Results are presented in Figure 3. As shown, our parallel update strategy enables updating a multi-module memory system with latency comparable to that of updating a single base memory module. This demonstrates the critical efficiency gains afforded by parallelization across the memory architecture.

3.5 Ablation Studies

We used the full Base and Long Subset from EB-ALFRED to validate RoboMemory’s effectiveness. We removed each component systematically and observed performance changes across task categories. We use the success rate as our metric. Results are shown in Table 2.

Long-term Memory Adding long-term memory significantly improved RoboMemory’s success rate. The experiment shows that it enables interactive environmental learning while attempting to complete tasks. The semantic memory learns low-level skills’ properties, such as in what circumstances an action may fail. The temporal memory records all task attempts (successful/failed), providing valuable experience at the task level and giving insight into how to complete a task successfully. This helps the RoboMemory predict action outcomes and avoid ineffective attempts. This ability indicates that the RoboMemory has an interactive environmental learning capability.

Spatial Memory Spatial memory is crucial for embodied agents, especially given that current pre-trained VLMs have limited spatial understanding ability. Our novel dynamic KG update algorithm enables KG-based spatial memory in dynamic environments. This spatial reasoning helps RoboMemory handle partially observable embodied settings.

Critic Module Table 2 shows performance without the critic module (55% vs 67% with full system). This drop highlights how the critic’s closed-loop planning adapts to dynamic environments. It helps RoboMemory recover from failures faster and handle unexpected situations better.

3.6 Real-world Robot Deployment

To evaluate RoboMemory’s interactive environmental learning capability in the real world, we designed a kitchen environment inspired by EB-ALFRED and EB-Habitat. The scene contains 5 navigable points, 8 interactive objects, and over 10 non-interactive (but potentially distracting) items. The environment is shown in Figure 4. In the real world, we use interactive environmental video recordings captured during action execution (rather than static snapshots taken after action completion) as RoboMemory’s input. This provides a more temporally coherent perception. We created three task categories (5 tasks each). Tasks are matched to EB-ALFRED’s Base subset (avg. oracle: 10–20 steps), though actual executions often exceed 20 steps due to search and error recovery.



Figure 4: Visualization of the experimental environment.

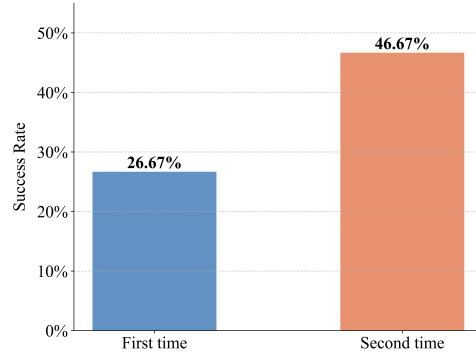


Figure 5: The improvement of RoboMemory after learning in the real world.

Due to search and error recovery, the robot often exceeds 20 steps per task. Additional hardware experiment details are in Appendix D.

To test the interactive environmental learning ability of RoboMemory, we run each task twice without clearing long-term memory between attempts. Success rates for first and second attempts are shown in Figure 5.

The second attempt showed significantly higher success rates. This proves RoboMemory’s long-term memory effectively guides subsequent tasks in real embodied environments. Key observations include: (1) Closed-loop error recovery: RoboMemory retries failed actions when possible, even if the low-level executor (VLA model) fails. (2) Spatial reasoning: RoboMemory remembers object locations and spatial relationships using its memory. (3) Interactive environmental learning: RoboMemory analyzes failure causes reasonably. These analyses guide future decisions. Detailed examples demonstrating these capabilities and further discussions are provided in Appendix E.

Moreover, we observed a significant drop in task success rates when deploying the agent with the Low-level Executor in real-world environments. This performance degradation primarily stems from the executor’s inherent limitations: (1) The VLA model exhibits unreliable instruction-following capabilities, frequently failing during grasping actions or selecting incorrect objects; (2) Pre-trained VLM models demonstrate inadequate video understanding - while capable of recognizing static objects, they struggle to interpret dynamic visual information such as action failures or state changes. These limitations collectively contribute to the reduced performance compared to simulated environments.

4 Conclusion and Future Work

In summary, RoboMemory, a brain-inspired multi-memory framework, facilitates long-horizon planning and interactive environmental learning in real-world embodied systems by addressing key challenges such as memory latency, task correlation capture, and planning loops. Experiments on EmbodiedBench demonstrate that RoboMemory outperforms state-of-the-art closed-source VLMs and agent frameworks, with ablation studies confirming the critical roles of the Critic module and spatial/long-term memory. Real-world deployment further validates its interactive learning capability through improved success rates in repeated tasks. Despite limitations arising from reasoning errors and executor dependence, RoboMemory provides a foundation for generalizable, memory-augmented agents, with future work aimed at refining reasoning and enhancing execution robustness.

A notable open challenge in hierarchical embodied agents, including RoboMemory, lies in the interface between high-level planners and low-level executors. Existing frameworks typically rely on language instructions to convey actions, yet some execution details (e.g., precise grasp points) are difficult to describe textually and are better captured through other modalities, such as vision. While our current work emphasizes long-term planning and interactive learning, future research may improve generalization by developing richer multimodal interactions between the agent and executor.

References

- [1] Saaket Agashe, Jiuzhou Han, Shuyu Gan, Jiachen Yang, Ang Li, and Xin Eric Wang. Agent s: An open agentic framework that uses computers like a human. *arXiv preprint arXiv:2410.08164*, 2024.
- [2] Anthropic. Claude 3.5 sonnet, 2024.
- [3] Shuai Bai, Keqin Chen, Xuejing Liu, Jialin Wang, Wenbin Ge, Sib0 Song, Kai Dang, Peng Wang, Shijie Wang, Jun Tang, et al. Qwen2. 5-vl technical report. *arXiv preprint arXiv:2502.13923*, 2025.
- [4] Johan Bjorck, Fernando Castañeda, Nikita Cherniadev, Xingye Da, Runyu Ding, Linxi Fan, Yu Fang, Dieter Fox, Fengyuan Hu, Spencer Huang, et al. Gr00t n1: An open foundation model for generalist humanoid robots. *arXiv preprint arXiv:2503.14734*, 2025.
- [5] Kevin Black, Noah Brown, Danny Driess, Adnan Esmail, Michael Equi, Chelsea Finn, Niccolo Fusai, Lachy Groom, Karol Hausman, Brian Ichter, et al. π_0 : A vision-language-action flow model for general robot control. *arXiv preprint arXiv:2410.24164*, 2024.
- [6] Neil Burgess, Eleanor A Maguire, and John O’Keefe. The human hippocampus and spatial and episodic memory. *Neuron*, 35(4):625–641, 2002.
- [7] Matthew Chang, Theophile Gervet, Mukul Khanna, Sriram Yenamandra, Dhruv Shah, So Yeon Min, Kavita Shah, Chris Paxton, Saurabh Gupta, Dhruv Batra, et al. Goat: Go to any thing. *arXiv preprint arXiv:2311.06430*, 2023.
- [8] Minghao Chen, Yihang Li, Yanting Yang, Shiyu Yu, Binbin Lin, and Xiaofei He. Automanual: Constructing instruction manuals by llm agents via interactive environmental learning. *Advances in Neural Information Processing Systems*, 37:589–631, 2024.
- [9] Xiaojun Chen, Shengbin Jia, and Yang Xiang. A review: Knowledge reasoning over knowledge graph. *Expert systems with applications*, 141:112948, 2020.
- [10] Zhe Chen, Weiyun Wang, Yue Cao, Yangzhou Liu, Zhangwei Gao, Erfei Cui, Jinguo Zhu, Shenglong Ye, Hao Tian, Zhaoyang Liu, et al. Expanding performance boundaries of open-source multimodal models with model, data, and test-time scaling. *arXiv preprint arXiv:2412.05271*, 2024.
- [11] Cheng Chi, Zhenjia Xu, Siyuan Feng, Eric Cousineau, Yilun Du, Benjamin Burchfiel, Russ Tedrake, and Shuran Song. Diffusion policy: Visuomotor policy learning via action diffusion. *The International Journal of Robotics Research*, page 02783649241273668, 2023.
- [12] Wonje Choi, Jinwoo Park, Sanghyun Ahn, Daehee Lee, and Honguk Woo. Nesyc: A neuro-symbolic continual learner for complex embodied tasks in open domains. *arXiv preprint arXiv:2503.00870*, 2025.
- [13] Google DeepMind. Introducing gemini 2.0: our new ai model for the agentic era, 2024.
- [14] Dayuan Fu, Biqing Qi, Yihuai Gao, Che Jiang, Guanting Dong, and Bowen Zhou. Msi-agent: Incorporating multi-scale insight into embodied agents for superior planning and decision-making. *arXiv preprint arXiv:2409.16686*, 2024.
- [15] Zipeng Fu, Tony Z Zhao, and Chelsea Finn. Mobile aloha: Learning bimanual mobile manipulation with low-cost whole-body teleoperation. *arXiv preprint arXiv:2401.02117*, 2024.
- [16] Yunfan Gao, Yun Xiong, Xinyu Gao, Kangxiang Jia, Jinliu Pan, Yuxi Bi, Yixin Dai, Jiawei Sun, Haofen Wang, and Haofen Wang. Retrieval-augmented generation for large language models: A survey. *arXiv preprint arXiv:2312.10997*, 2(1), 2023.
- [17] Marc Glocker, Peter Hönig, Matthias Hirschmanner, and Markus Vincze. Llm-empowered embodied agent for memory-augmented task planning in household robotics. *arXiv preprint arXiv:2504.21716*, 2025.

- [18] Bernal Jiménez Gutiérrez, Yiheng Shu, Yu Gu, Michihiro Yasunaga, and Yu Su. Hipporag: Neurobiologically inspired long-term memory for large language models. *arXiv preprint arXiv:2405.14831*, 2024.
- [19] Edward J Hu, Yelong Shen, Phillip Wallis, Zeyuan Allen-Zhu, Yuanzhi Li, Shean Wang, Lu Wang, Weizhu Chen, et al. Lora: Low-rank adaptation of large language models. *ICLR*, 1(2):3, 2022.
- [20] Yafei Hu, Quanting Xie, Vidhi Jain, Jonathan Francis, Jay Patrikar, Nikhil Keetha, Seungchan Kim, Yaqi Xie, Tianyi Zhang, Hao-Shu Fang, et al. Toward general-purpose robots via foundation models: A survey and meta-analysis. *arXiv preprint arXiv:2312.08782*, 2023.
- [21] Aaron Hurst, Adam Lerer, Adam P Goucher, Adam Perelman, Aditya Ramesh, Aidan Clark, AJ Ostrow, Akila Welihinda, Alan Hayes, Alec Radford, et al. Gpt-4o system card. *arXiv preprint arXiv:2410.21276*, 2024.
- [22] Moo Jin Kim, Karl Pertsch, Siddharth Karamcheti, Ted Xiao, Ashwin Balakrishna, Suraj Nair, Rafael Rafailov, Ethan Foster, Grace Lam, Pannag Sanketi, et al. Openvla: An open-source vision-language-action model. *arXiv preprint arXiv:2406.09246*, 2024.
- [23] Mingcong Lei, Ge Wang, Yiming Zhao, Zhixin Mai, Qing Zhao, Yao Guo, Zhen Li, Shuguang Cui, Yatong Han, and Jinke Ren. Clea: Closed-loop embodied agent for enhancing task execution in dynamic environments. *arXiv preprint arXiv:2503.00729*, 2025.
- [24] Bill Yuchen Lin, Yicheng Fu, Karina Yang, Faeze Brahman, Shiyu Huang, Chandra Bhagavatula, Prithviraj Ammanabrolu, Yejin Choi, and Xiang Ren. Swiftsage: A generative agent with fast and slow thinking for complex interactive tasks. *Advances in Neural Information Processing Systems*, 36, 2024.
- [25] Kourosh Maboudi, Bapun Giri, Hiroyuki Miyawaki, Caleb Kemere, and Kamran Diba. Retuning of hippocampal representations during sleep. *Nature*, 629(8012):630–638, 2024.
- [26] Meta. Llama 3.2: Revolutionizing edge ai and vision with open, customizable models, 2024.
- [27] David Milner. Cognitive neuroscience: the biology of the mind and findings and current opinion in cognitive neuroscience. *Trends in cognitive sciences*, 2(11):463, 1998.
- [28] OpenAI. Gpt-4o mini: advancing cost-efficient intelligence, 2024.
- [29] Charles Packer, Sarah Wooders, Kevin Lin, Vivian Fang, Shishir G. Patil, Ion Stoica, and Joseph E. Gonzalez. MemGPT: Towards llms as operating systems. *arXiv preprint arXiv:2310.08560*, 2023.
- [30] Joon Sung Park, Joseph O’Brien, Carrie Jun Cai, Meredith Ringel Morris, Percy Liang, and Michael S Bernstein. Generative agents: Interactive simulacra of human behavior. In *Proceedings of the 36th annual acm symposium on user interface software and technology*, pages 1–22, 2023.
- [31] Lucy Xiaoyang Shi, Brian Ichter, Michael Equi, Liyiming Ke, Karl Pertsch, Quan Vuong, James Tanner, Anna Walling, Haohuan Wang, Niccolo Fusai, et al. Hi robot: Open-ended instruction following with hierarchical vision-language-action models. *arXiv preprint arXiv:2502.19417*, 2025.
- [32] Noah Shinn, Federico Cassano, Ashwin Gopinath, Karthik Narasimhan, and Shunyu Yao. Reflexion: Language agents with verbal reinforcement learning. *Advances in Neural Information Processing Systems*, 36, 2024.
- [33] Chan Hee Song, Jiaman Wu, Clayton Washington, Brian M Sadler, Wei-Lun Chao, and Yu Su. Llm-planner: Few-shot grounded planning for embodied agents with large language models. In *Proceedings of the IEEE/CVF international conference on computer vision*, pages 2998–3009, 2023.
- [34] Huajie Tan, Xiaoshuai Hao, Cheng Chi, Minglan Lin, Yaoxu Lyu, Mingyu Cao, Dong Liang, Zhuo Chen, Mengsi Lyu, Cheng Peng, et al. Roboos: A hierarchical embodied framework for cross-embodiment and multi-agent collaboration. *arXiv preprint arXiv:2505.03673*, 2025.

- [35] Weihao Tan, Wentao Zhang, Xinrun Xu, Haochong Xia, Ziluo Ding, Boyu Li, Bohan Zhou, Junpeng Yue, Jiechuan Jiang, Yewen Li, et al. Cradle: Empowering foundation agents towards general computer control. *arXiv preprint arXiv:2403.03186*, 2024.
- [36] Gemini Team, Petko Georgiev, Ving Ian Lei, Ryan Burnell, Libin Bai, Anmol Gulati, Garrett Tanzer, Damien Vincent, Zhufeng Pan, Shibo Wang, et al. Gemini 1.5: Unlocking multimodal understanding across millions of tokens of context. *arXiv preprint arXiv:2403.05530*, 2024.
- [37] Qwen Team. Qwen2.5: A party of foundation models, September 2024.
- [38] Guanzhi Wang, Yuqi Xie, Yunfan Jiang, Ajay Mandlekar, Chaowei Xiao, Yuke Zhu, Linxi Fan, and Anima Anandkumar. Voyager: An open-ended embodied agent with large language models. *arXiv preprint arXiv:2305.16291*, 2023.
- [39] Colin White, Samuel Dooley, Manley Roberts, Arka Pal, Ben Feuer, Siddhartha Jain, Ravid Shwartz-Ziv, Neel Jain, Khalid Saifullah, Siddartha Naidu, et al. Livebench: A challenging, contamination-free llm benchmark. *arXiv preprint arXiv:2406.19314*, 2024.
- [40] Rui Yang, Hanyang Chen, Junyu Zhang, Mark Zhao, Cheng Qian, Kangrui Wang, Qineng Wang, Teja Venkat Koripella, Marziyeh Movahedi, Manling Li, et al. Embodiedbench: Comprehensive benchmarking multi-modal large language models for vision-driven embodied agents. *arXiv preprint arXiv:2502.09560*, 2025.
- [41] Zhejian Yang, Yongchao Chen, Xueyang Zhou, Jiangyue Yan, Dingjie Song, Yinyao Liu, Yuting Li, Yu Zhang, Pan Zhou, Hechang Chen, et al. Agentic robot: A brain-inspired framework for vision-language-action models in embodied agents. *arXiv preprint arXiv:2505.23450*, 2025.
- [42] Shunyu Yao, Jeffrey Zhao, Dian Yu, Nan Du, Izhak Shafran, Karthik Narasimhan, and Yuan Cao. React: Synergizing reasoning and acting in language models. *arXiv preprint arXiv:2210.03629*, 2022.
- [43] Haoqi Yuan, Yu Bai, Yuhui Fu, Bohan Zhou, Yicheng Feng, Xinrun Xu, Yi Zhan, Börje F Karlsson, and Zongqing Lu. Being-0: A humanoid robotic agent with vision-language models and modular skills. *arXiv preprint arXiv:2503.12533*, 2025.
- [44] Hongxin Zhang, Weihua Du, Jiaming Shan, Qinhong Zhou, Yilun Du, Joshua B Tenenbaum, Tianmin Shu, and Chuang Gan. Building cooperative embodied agents modularly with large language models. *arXiv preprint arXiv:2307.02485*, 2023.
- [45] Yanzhao Zhang, Mingxin Li, Dingkun Long, Xin Zhang, Huan Lin, Baosong Yang, Pengjun Xie, An Yang, Dayiheng Liu, Junyang Lin, et al. Qwen3 embedding: Advancing text embedding and reranking through foundation models. *arXiv preprint arXiv:2506.05176*, 2025.
- [46] Andrew Zhao, Daniel Huang, Quentin Xu, Matthieu Lin, Yong-Jin Liu, and Gao Huang. Expel: Llm agents are experiential learners. In *Proceedings of the AAAI Conference on Artificial Intelligence*, volume 38, pages 19632–19642, 2024.
- [47] Tony Z Zhao, Vikash Kumar, Sergey Levine, and Chelsea Finn. Learning fine-grained bimanual manipulation with low-cost hardware. *arXiv preprint arXiv:2304.13705*, 2023.
- [48] Jinguo Zhu, Weiyun Wang, Zhe Chen, Zhaoyang Liu, Shenglong Ye, Lixin Gu, Hao Tian, Yuchen Duan, Weijie Su, Jie Shao, et al. Internvl3: Exploring advanced training and test-time recipes for open-source multimodal models. *arXiv preprint arXiv:2504.10479*, 2025.

A Related Work

A.1 VLM/LLM-based Agentic Frameworks in Embodied Tasks

The rapid advancement of VLMs/LLMs has led to diverse agent frameworks in embodied environments [42, 33, 24]. Embodied tasks involve partial observability and long-horizon planning, requiring memory systems to retain context. Some use time-ordered context buffers for short-term memory (due to VLMs/LLMs’ limited long-context processing) [42, 29]; others adopt experience buffers as long-term semantic memory [14, 32]. For long-duration tasks, skill libraries serve as procedural memory, with agents accumulating skills via interaction [38, 35]. However, in real-world settings, the low-level executor may fail to complete the task, making it challenging to construct a reusable, code-based skill library. So, explicit procedural memory still needs to be improved in real-world settings. Moreover, Recent efforts integrate diverse memories [44, 35, 1] but focus on virtual/GUI environments, leaving real-world multi-modal memory support for long-term planning under-explored.

A.2 Vision Language Action Model

Current work on VLA models uses imitation learning to output low-level controls from language and visuals [5, 47, 4, 22] but is limited to tabletop tasks and single actions, restricting long-horizon planning. VLAs lack long-term execution abilities, while high-level agents excel at planning. Recent works combine high-level frameworks with VLA executors, some augmented with simple memory [31, 34, 43, 41] for longer tasks. However, real-world robots need more sophisticated memory to handle continuous multi-task operations over extended periods.

A.3 Memory Frameworks

Many previous works improve long-term planning via memory systems: Voyager [38] uses a skill library in Minecraft but lacks diverse memory types; CoELA [44] includes procedural, semantic, and episodic memory with a task-specific 2D map; MSI-Agent [14] utilizes insight as long-term memory for in-task learning. Hippo Retrieval Augmented Generation (RAG) [18] mimics the hippocampus and introduces KGs as long-term memory indices [6, 9], enhancing retrieval. However, the previous approach is mainly focused on constructing a KG with a static long context, such as a book, but it is hard to update the graph. We need to update the information in KG for the embodied task. Our approach builds a more general LLM-based memory system using a dynamic KG like Hippo RAG, which is designed for embodied tasks. Furthermore, we summarize the differences among different memory systems in previous work. The comparison is shown in the Table 3.

Table 3: Comparison of Memory-Related Methods in Embodied Agent

Method	Multimodal	Episodic	Semantic	Spatial	Temporal	Procedural	Memory Implementation	Real Robot
NeSyC [12]	✓		✓		✓		Symbolic logic rules	✓
Reflexion [32]			✓		✓		Buffer	
Voyager [38]						✓	RAG	
MSI-Agent [14]			✓		✓		Database, RAG	
CoELA [44]	✓	✓	✓			✓	Top-down semantic map	
Cradle [35]	✓	✓			✓	✓	RAG	
Agent-S [11]	✓	✓	✓		✓		RAG	
Expel [46]			✓		✓		Buffer	
AutoManual [8]		✓	✓			✓	Buffer	
HiRobot [31]	✓						/	✓
Being-0 [43]	✓	✓			✓		Buffer	✓
RoboOS [34]	✓			✓	✓		Scene graph, database	✓
RoboMemory (Ours)	✓	✓	✓	✓	✓		RAG,KG	✓

B Additional Experiments

B.1 Error Analysis

We summarize the common errors of RoboMemory in the previous experiments. We classify errors into three main types: planning errors, reasoning errors, and perception errors.

The planning errors occur when the planner fails to generate correct actions. The reasoning errors occur when the planner and critic cannot properly process input information (including current observations and memory), even when the input is correct. Perception errors occur when incorrect information is provided to the planner-critic module.

We analyze RoboMemory trajectories for failed tasks. We identify error types based on the above definitions. A single task may contain multiple errors. We calculate the occurrence probability of each error type to show RoboMemory’s strengths and weaknesses. The results are shown in Figure 6.

We can observe that among all error types, the planning errors are the most common. This means that even though the memory modules can provide comprehensive information about the RoboMemory agent’s previous experience and spatial and temporal memory for the current task, the planner module may still not provide good action plans. This may be due to the capability of the pretrained base model.

The most common perception error is the hallucination error. We can observe that although some hallucinations can be handled by the critic module or memory information, there are still some cases in which the planner ignores all insights from memory and critic and fails to complete the task.

The detailed examples and discussions are provided in Appendix E.



Figure 6: The reason why RoboMemory failed to complete the task.

B.2 Evaluate on EB-Habitat

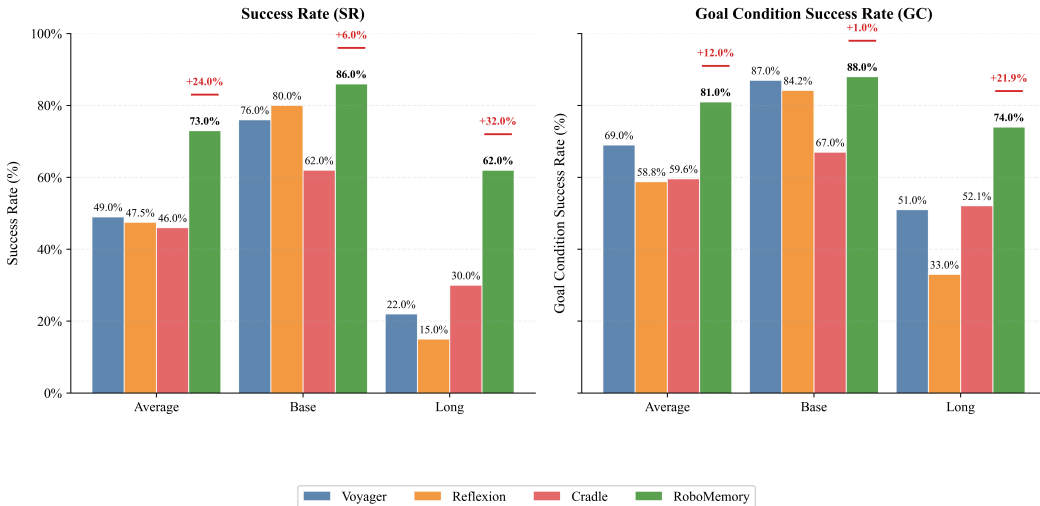


Figure 7: Comparison of Success Rates (SR) and Goal Condition Success Rates (GC) across difficulty levels between RoboMemory and baseline methods on EB-Habitat.

Similar to EB-ALFRED, we also deploy RoboMemory to EB-Habitat. Both EB-Habitat and EB-HALFRED are subsets of EmbodiedBench. We evaluate our model on the Base and Long subsets. Each subset contains 50 different trails. The results are shown in Figure 7.

The results demonstrate that our RoboMemory can adapt well to different environments. It achieves significant improvements over the baseline across various settings. On average, the success rate

increases by 24% compared to the SOTA Multi-Agent Method. The goal-conditioned success rate improves by 12%.

These improvements indicate that RoboMemory enhances the agent’s embodied intelligence in various environments. The key factor is its complete memory system.

B.3 Additional Efficiency analysis

We analyze the evolution of the spatial KG during long trajectories in EB-ALFRED, focusing on the first 20 iterations (with 95% confidence intervals). As shown in Figure 8, the total number of spatial relationships in the KG (red line) increases gradually over iterations as RoboMemory is exploring the environment. In contrast, the number of relationships retrieved for update at each iteration (blue line) remains relatively stable, typically ranging around 10 edges per iteration. This stability is achieved because our method only updates a local subgraph relevant to the current observation.

We define the retrieval ratio as the proportion of relationships updated at each iteration relative to the total number of relationships in the KG. As shown in Figure 8, this ratio (illustrated by gray bars) decreases steadily from 76% initially to 28% at iteration 20. This trend indicates that, as the KG grows, each update affects a progressively smaller fraction of the entire graph. This demonstrates that our spatial KG update mechanism effectively localizes modifications, ensuring computational efficiency and mitigating interference through context-aware incremental updates.

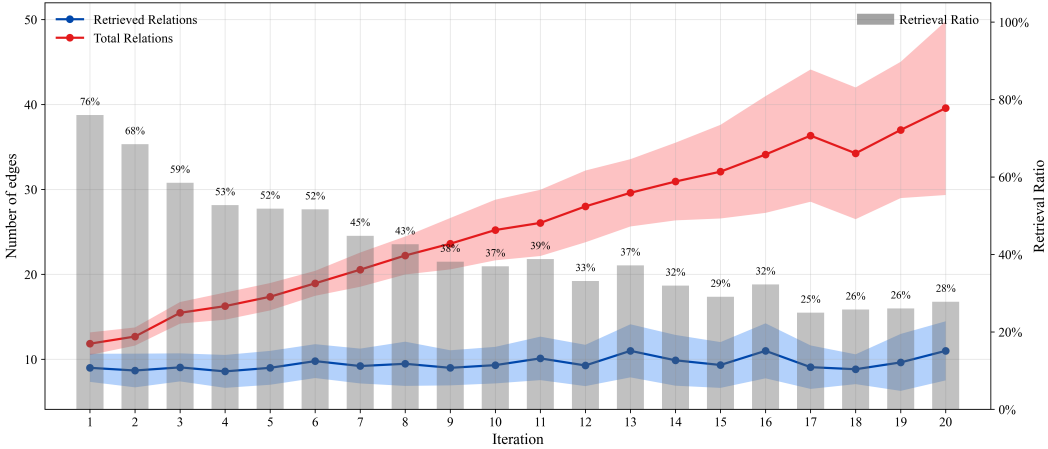


Figure 8: Average relationships related to update in spatial memory in each step.

C Dynamic Spatial Memory Update Algorithm

C.1 Detailed Algorithm of Spatial KG Update

Spatial Memory is a dynamically updated KG-based module designed to overcome agents’ limitations in spatial reasoning. Specifically, our Spatial Memory is formulated as a directed KG $G = (V, E)$, where V denotes the set of all objects in the environment. Each object is a vertex in the KG. Each object’s name is encoded into a single semantic embedding vector via a pretrained embedding model [45]. The edge set E captures spatial relationships between objects, each represented as a triple (e.g., $[obj_1, relationship, obj_2]$). To update the Spatial KG, we need to continuously extract new relationships from current observations and update the old relationships in the Spatial KG. We use a VLM-based conflict resolver to address this problem. However, the more relationships provided to the conflict resolver, the more time it needs to update the KG. So we need to update relationships that are only related to the current situation. We design an algorithm that retrieves a sub-graph of KG that includes all vertices related to the current situation and both old and new relationships among them. We provide the sub-graph and new relationships to the conflict resolver. We need the conflict resolver to update the sub-graph based on information from the new relationships. The algorithm is shown in Algorithm 1.

Algorithm 1 Retrieval-based Incremental Knowledge Graph Update Algorithm

Require: New spatial knowledge graph $G_{\text{new}} = (V_{\text{new}}, E_{\text{new}})$, main spatial knowledge graph $G = (V, E)$, queries $q \in Q$, entity & query embeddings $\mathcal{E} : V \cup Q \rightarrow \mathbb{R}^d$, maximum number of retrieved vertices n , maximum k hops k , vlm-base conflict resolver $\text{ResolveConflict}(\cdot)$

Ensure: Updated consistent knowledge graph G'

- 1: $V_{\text{similar}} \leftarrow \bigcup_{q \in Q} \text{TopK}_n(\{v \in V \mid \text{cosine_sim}(\mathcal{E}(q), \mathcal{E}(v))\})$ {For each query entity q , retrieve its top- n most similar vertices in G by cosine similarity of embeddings; take the union over all $q \in Q$.}
 - 2: $V_{\text{expand}} \leftarrow \text{K-hop}_k(V_{\text{similar}}, G)$ {all nodes within k hops from any node in V_{similar} }
 - 3: $V_{\text{retrieved}} \leftarrow V_{\text{similar}} \cup V_{\text{expand}}$
 - 4: $V_{\text{merged}} \leftarrow V_{\text{retrieved}} \cup V_{\text{new}}$
 - 5: $G_{\text{union}} \leftarrow (V \cup V_{\text{new}}, E \cup E_{\text{new}})$ {Combine the main graph and new observations into a unified graph.}
 - 6: $G_{\text{local}} \leftarrow \text{InducedSubgraph}(V_{\text{merged}}, G_{\text{union}})$ {Extract the subgraph induced by V_{merged} , containing all old and new edges among these nodes.}
 - 7: $G_{\text{updated}} \leftarrow \text{ResolveConflict}(G_{\text{local}}, G_{\text{new}})$ {based on G_{new} , VLM update the relationship among different vertices in G_{local} }
 - 8: $G' \leftarrow (G \setminus G_{\text{local}}) \cup G_{\text{updated}}$ {Replace the old subgraph in G with the conflict-resolved updated subgraph.}
 - 9: Remove isolated vertices from G'
 - 10: **return** G'
-

To update G , we make use of the information provided by the step summarizer and query generator from the information preprocessor introduced in Sec. 2.1. First, a pretrained VLM-based Relation Retriever extracts the latest spatial relationships $G_{\text{new}} = (V_{\text{new}}, E_{\text{new}})$ from the information provided by the step summarizer, which records high-level information in the current observation. Next, natural language queries (represented as $q \in Q$) (provided by the query generator) are used to retrieve relevant object vertices from G via cosine similarity search. We select the top n similar vertices compared with the query. These vertices are represented by V_{similar} .

Spatial KG maintains the relationships among different objects, so if we want to retrieve spatial information from spatial KG, we need to search for other objects that are related to the objects we observed in the current observation. In this way, we not only remember objects we can see, but also know the spatial information of the objects we cannot see. So we choose the k-hop algorithm to expand V_{similar} using a K-hop neighborhood algorithm to capture contextually related objects. The K-hop algorithm is represented as $\text{K-hop}_k(V, G)$, which returns all vertices reachable within $\leq k$ hops from any vertices in V . The retrieved vertices are V_{expand} . We combine the vertices retrieved by cosine similarity and their K-hop neighbors to $V_{\text{retrieved}}$.

However, we need to resolve the conflict between new and old relationships. So $V_{\text{retrieved}}$ and the relationships among $V_{\text{retrieved}}$ is not enough. We need new vertices and relationships involved in the graph we provided to the VLM-based conflict resolver. To extract all vertices and relationships for the VLM-based conflict resolver and relationships, we not only need the relationships from KG (old information) and G_{new} , which represent new information. We need to connect old information and new information. To achieve this goal, we merge G_{new} to G , which add new edges and vertices to G . We denote the merged KG as G_{union} . In G_{union} , we mix out-of-date and latest information. Then, we extract an induced sub-graph of $V_{\text{merged}} = V_{\text{retrieved}} \cup V_{\text{new}}$ from G_{union} . As both vertices from old graph G and new graph is mixed in V_{merged} and both edges from old and new graph is in G_{union} , the retrieved induced sub-graph G_{local} contains all out-of-date and latest relationships among vertices that is related to current situation.

As G_{local} contains all out-of-date and latest relationships and those relationships may have conflicts, a VLM-based conflict resolver (represented as $\text{ResolveConflict}(\cdot)$) is designed to resolve conflicts in G_{local} , and make sure that the relationship is the latest. The conflict resolver will take in G_{new} and G_{local} , where G_{local} is the graph waiting for update and G_{new} provide update signal. The VLM-based conflict resolver will perform necessary updates such as adding vertices or inserting, deleting, or modifying relationships in G_{local} based on G_{new} . The reconciled subgraph is then merged back into G , and any vertices that have lost all connections to other vertices during the update are pruned.

Satisfies the following upper bound:

$$|\mathcal{N}_K(\mathcal{S})| \leq \begin{cases} M \cdot \frac{D^{K+1} - 1}{D - 1}, & \text{if } D > 1, \\ M \cdot (K + 1), & \text{if } D = 1. \end{cases}$$

Proof. For any vertex $s \in \mathcal{S}$, the number of distinct vertices reachable from s within i hops is at most D^i , assuming the worst-case scenario where each vertex encountered has the maximum out-degree D , and all neighbors are distinct and non-overlapping.

Thus, the size of the K -hop neighborhood of a single vertex satisfies:

$$|\mathcal{N}_K(s)| \leq \sum_{i=0}^K D^i = \begin{cases} \frac{D^{K+1} - 1}{D - 1}, & \text{if } D > 1, \\ K + 1, & \text{if } D = 1. \end{cases}$$

Since there are M such source vertices and assuming no overlaps between their K -hop neighborhoods (worst case), the union size satisfies:

$$|\mathcal{N}_K(\mathcal{S})| \leq M \cdot |\mathcal{N}_K(s)|.$$

Substituting the bound on $|\mathcal{N}_K(s)|$ gives the result. \square

Theorem 2 (Upper Bound for K -hop Vertex Extraction in Normalized Directed Graphs). *Let $G = (V, E)$ be a finite directed graph with $|V| = n$ vertices. Assume the maximum out-degree is at most $D_{\max} = Dn$, and the maximum in-degree is at most $N_{\max} = Nn$, where $D, N \in (0, 1]$ are constants. Let $\mathcal{S} \subseteq V$ be a set of M source vertices. Define $\mathcal{N}_K(\mathcal{S})$ as the union of all vertices reachable from \mathcal{S} via paths of length at most K , using only outgoing edges. Then the number of extracted vertices satisfies:*

$$|\mathcal{N}_K(\mathcal{S})| \leq \min \left\{ n, M \cdot \frac{(Dn)^{K+1} - 1}{Dn - 1} \right\}.$$

In particular, when $Dn \gg 1$, we have the approximation:

$$|\mathcal{N}_K(\mathcal{S})| \lesssim M \cdot (Dn)^K.$$

Proof. For each vertex $s \in \mathcal{S}$, the maximum number of reachable vertices within i -hops is at most $(Dn)^i$ under the assumption of maximum out-degree and no overlap.

Summing over hops from 0 to K , we get for each root:

$$|\mathcal{N}_K(s)| \leq \sum_{i=0}^K (Dn)^i = \frac{(Dn)^{K+1} - 1}{Dn - 1}.$$

Assuming no overlap among the M source vertex expansions (worst case), we have:

$$|\mathcal{N}_K(\mathcal{S})| \leq M \cdot \frac{(Dn)^{K+1} - 1}{Dn - 1}.$$

Since the total number of vertices in the graph is n , this quantity is also trivially bounded above by n , yielding the result. \square

D Additional Environment settings

D.1 EB-ALFRED and EB-Habitat

We adopt the same environment parameters as in EmbodiedBench. The maximum steps per task are set to 30, with image inputs of size 500×500 . The temporal memory buffer length is set to 3.

However, we modified the action formats of EB-ALFRED and EB-Habitat to simulate real-world scenarios better. Specifically, we define different action APIs (Python functions), where each action takes an object parameter indicating its target. We extract all possible objects from the environment as inputs to the Agent. The Agent must select appropriate actions and object parameters based on task requirements. Compared to the original interaction method in EmbodiedBench (which enumerates all possible actions, including both action names and target objects, and requires the Agent to choose), our approach offers greater flexibility. The detailed action APIs are presented in Table 4.

Since EB-ALFRED and EB-Habitat provide comprehensive high-level action APIs, we do not employ the VLA-Based Low-Level Executor in these environments. Instead, we utilize the built-in low-level controllers from EmbodiedBench.

D.2 Real-world experiments

Table 4: Robot Action Command For different environments

Action Type	EB-ALFRED	EB-Habitat	Real World
Navigation	find(obj)	navigate(point)	navigate_to(point)
Pick Up Object	pick_up(obj)	pick(obj)	pick_up(obj)
Drop to Ground	drop()	-	-
Place to Receptacle	put_down()	place(rec)	put_down_to(rec)
Open Object	open(obj)	open(obj)	open(obj)
Close Object	close(obj)	close(obj)	close(obj)
Turn On	turn_on(obj)	-	turn_on(obj)
Turn Off	turn_off(obj)	-	turn_off(obj)
Slice Object	slice(obj)	-	-
Task Complete	-	-	task_complete()

We construct a common kitchen scenario to evaluate the RoboMemory framework’s interactive environmental learning capabilities in real-world settings. Using Mobile ALOHA [15] as our physical robotic platform, we design three categories of tasks: (1) Pick up & put down: The agent must locate a specified object among all possible positions and place it at a designated location. This task tests the model’s basic object-searching and planning abilities. (2) Pick up, operate & put down: Building upon the first task, the agent must additionally perform operations such as heating or cleaning the object. This task requires longer-term planning, which is crucial in embodied environments. (3) Pick up, gather & put down: The agent must place specified objects into a movable container and then move the container to a target location. This task evaluates the agent’s understanding of object relationships, requiring it to remember the positions of at least two objects (the container and the target item) and their spatial relationship. For each type of task, we design 5 tasks. So our experiments include 15 long-term real-world tasks.

To adapt to the real-world setup, we define high-level action APIs similar to those in EB-ALFRED and EB-Habitat. Additionally, we train a VLA-based model to execute tasks according to our action APIs. The detailed action APIs are presented in Table 4.

For the low-level executor, we use one main camera and two arm-mounted cameras as input, each with a resolution of 640×480 . The temporal memory buffer length is set to 3.

In our experiments, we set the maximum steps per task to 25. We also provide an API for actively terminating tasks. Since real-world environments lack direct success/failure feedback, RoboMemory must autonomously determine task completion. To prevent excessively long task execution, we enforce termination after 25 steps if no success is achieved. A single main camera (640×480 resolution) records video during action execution as input for RoboMemory’s higher-level processing.

D.3 Training Details of Low-Level Executor

We use the π_0 model as our foundation model. We collected 1,040 data samples over 10 types of tasks for fine-tuning. We use LoRA fine-tuning to save resources during fine-tuning. The specific fine-tuning parameters and action types are given in Table 5. For tasks involving both pick-up and place actions, we split these tasks into separate pick-up and place actions. These are then treated as two distinct data samples during training. The separation of pick-up and place action allows the

Table 5: Dataset statistics and training hyperparameters for robotic manipulation tasks.

Dataset Statistics		Training Configuration	
Action Type	#Episodes	Parameter	Value
Turning on/off faucet	142	Optimizer	AdamW
Picking up & Placing basket on counter	63	Batch size	32×6
Picking up & Placing basket in sink	72	Training steps	10,000
Picking up & Placing banana into basket	114	Learning rate	6.12×10^{-5}
Throwing bottle into trash bin	132	warm up step	500
Placing gum box on dish	120	LoRA Configuration	
Picking up & Placing cup on plate	51	rank	16
Picking up & Placing dish into sink	69	α	16
Throwing paper ball into trash bin	135	Resource Usage	
Open/close oven	142	GPU	A100-80GB \times 6
Total episodes	1040	Training time	12 hours

VLA to carry an object in its hand. For training, we used a server with six A100-80GB GPUs. The total training time was 12 hours.

Besides, we use the built-in LiDAR SLAM system of the Mobile ALOHA robot base as the navigation action actuator. We define five typical navigation points, similar to EB-Habitat. We used SLAM to navigate between these navigation points.

D.4 Hyperparameters of RoboMemory

In this section, we describe the hyperparameter settings for the upper brain of RoboMemory: the information preprocessor and the Comprehensive Embodied Memory. Importantly, we use a unified set of hyperparameters across all experimental settings, including EB-ALFRED, EB-Habitat, and real-world deployments.

The information preprocessor consists of two components: a step summarizer and a query generator. Given multimodal inputs at each step, the step summarizer produces a single natural language description, while the query generator concurrently formulates 4 – 5 distinct natural language queries.

The Comprehensive Embodied Memory integrates four memory modules: Temporal, Spatial, Semantic, and Episodic Memory. The Temporal Memory is implemented as a fixed-size buffer with a maximum capacity of 4 entries. For Spatial Memory, during similarity-based retrieval, we first identify the top $N = 3$ most relevant vertices and then perform a K-hop graph traversal with $K = 2$. The Episodic Memory retrieves the top $N = 5$ most relevant past experiences for each query. The Semantic Memory maintains hierarchical summaries at both the action and task levels; during retrieval, it returns $N_s = 2$ action-level and $N_t = 2$ task-level summaries. Furthermore, memory updates (e.g., insertion, modification, or deletion) are applied only to the top $N_{\text{update}} = 10$ most relevant entries in the Semantic Memory to ensure efficiency and coherence.

E Supplementary Examples for Qualitative Analysis

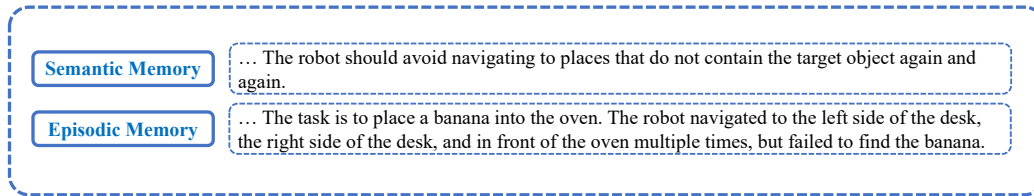
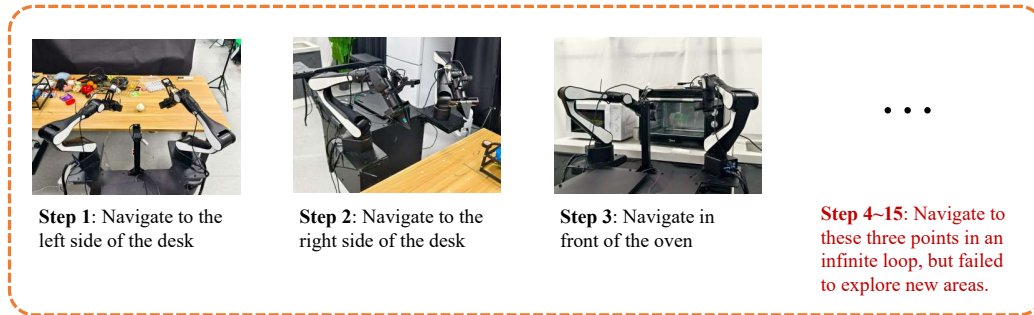
E.1 Real World

In Figure 10, we demonstrate an example of RoboMemory learning through trial and error in a real-world environment. Our task is “place a banana into the oven.” This task required RoboMemory to complete the objectives of finding the banana, picking it up, and transporting it to the oven. We observed that RoboMemory became stuck in an infinite loop during the first attempt. The banana was randomly placed on the “kitchen counter,” but RoboMemory overlooked this navigation target and remained trapped, exploring other navigation targets instead.

However, based on this bad attempt, the semantic memory summarized that the robot should not repeatedly search in locations where the “banana” could not be found. Meanwhile, the episodic memory recorded what RoboMemory had done and the outcomes during the first attempt. Based on

Task: Place banana into the oven

The first time



The second time

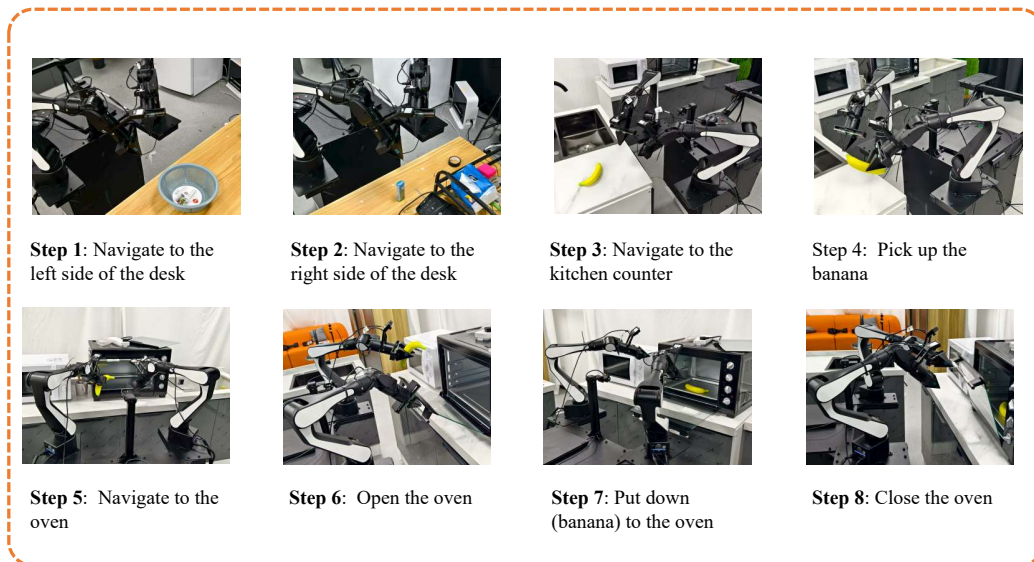


Figure 10: Case that a task is failed, but the experience can help RoboMemory to succeed in the next try.

the information provided by semantic and episodic memory, in the second attempt, RoboMemory recognized that it had not previously tried navigating to the “kitchen counter.” After attempting this, it successfully completed the task. This example illustrates the role of RoboMemory’s long-term memory.

We also provide an example that completes the task in the first attempt. The example is shown in Figure 11. This example demonstrates that the RoboMemory has the ability to handle some relatively complex tasks in the real world. The task in this example is “Place a box of gum into the basket and put the basket on the kitchen counter”. Because two objects in different positions are

Task: Place a box of gum into the basket and put the basket to the kitchen counter



Figure 11: Case that a task is successful.

involved in this task, RoboMemory has to memorize the position of at least one object to achieve the goal. With the help of the spatial memory, RoboMemory completes the task successfully.

E.2 EB-ALFRED

We select three examples in EB-ALFRED to show the errors that RoboMemory may encounter and the reasons why or why not RoboMemory can achieve the goal.

E.2.1 Successful example

We select a successful example to show how RoboMemory performed in the EB-ALFRED environment. The example trajectory is shown in Figure 12.

The task of this example is “set a plate with a spoon on it on the kitchen table”. However, in step 10, the Planner seems to ignore the temporal information from memory modules. RoboMemory thinks that it still needs to pick up the spoon (even though it has already placed a spoon in the plate). However, with the help of the critic, it finally becomes aware that picking up another spoon is redundant, so RoboMemory goes back to the current trajectory and successfully completes the task at the end.

In this example, RoboMemory successfully overcame the hallucination and eventually achieved the goal. This example demonstrates that the critic module can help RoboMemory to overcome error cases.

E.2.2 Failed example

We demonstrate a representative example of the Critical Error. The example trajectory is shown in Figure 13. In this example, the task involves slicing and heating a tomato and moving the heated tomato slice to the trash can. Initially, RoboMemory successfully sliced the tomato with a knife. But when the planner plans the whole sequence, it forgets to drop the knife before picking up the tomato (this is necessary because in EB-ALFRED, the robot can only hold one object at a time). The critic and the planner should notice this situation and ask the critic to replan, as RoboMemory failed to pick up a tomato slice. However, the critic module ignores this issue, and thus, after it heats the knife instead of a tomato slice, it stacks in an infinite loop.

Besides, we provide another example demonstrating a representative failure caused by inaccurate action planning. The example trajectory is shown in Figure 14. In the trajectory, RoboMemory is

Task: Set plate with a spoon in it on the kitchen table

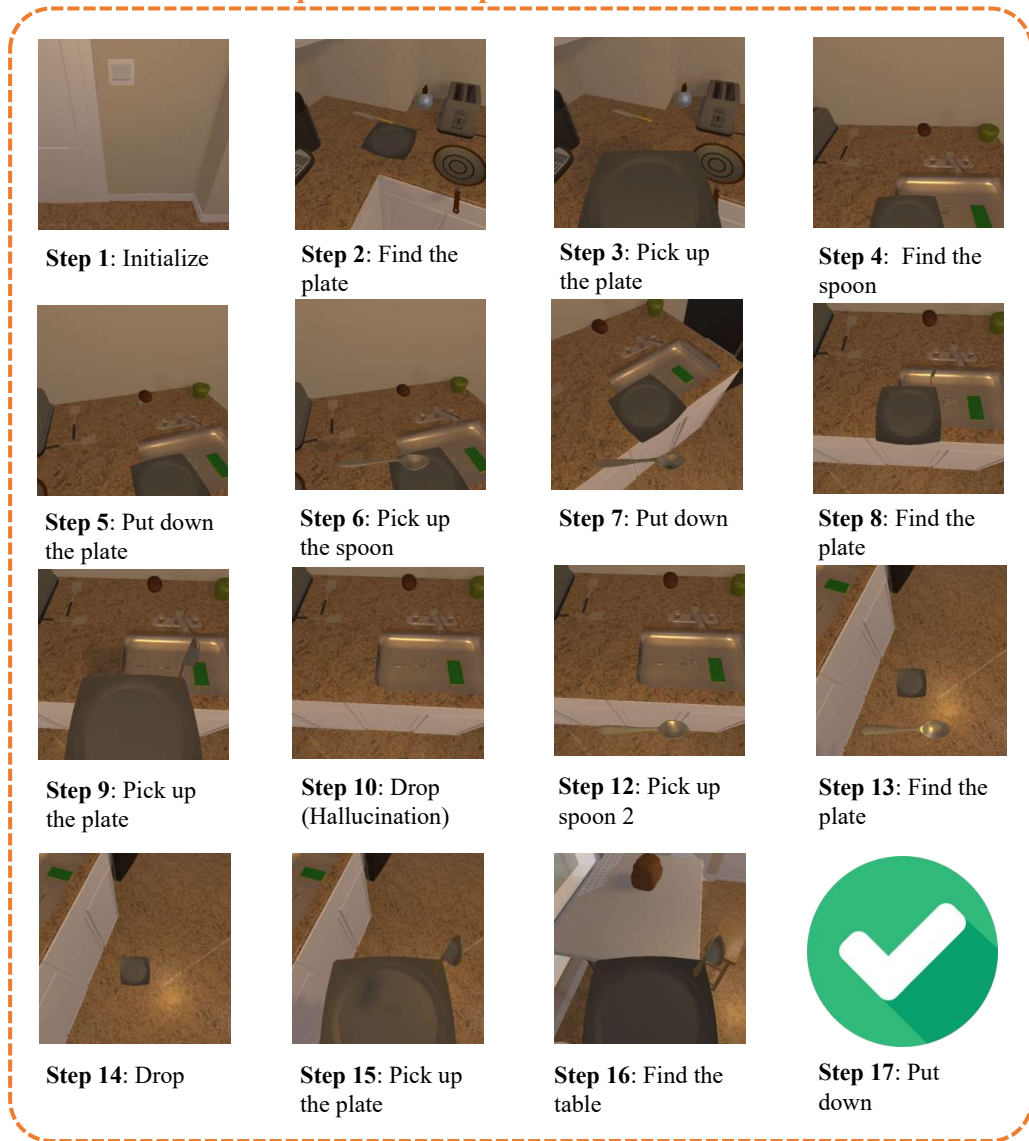


Figure 12: Case that a task is successful with the help of the critic and spatial memory modules.

asked to place two CDs into the drawer. However, at step 6, the robot failed to select correct CD object. In this experiment, RoboMemory has already put CD_2 into the drawer, but it keeps picking up CD_2 even though the memory has clearly indicated that CD_2 has already been put down. So we classify this as inaccurate action error. This indicates that the planner failed to comprehensively integrate information from both the memory and information-gathering modules, resulting in inaccurate action planning.

Task: Cook a sliced tomato and throw it in the trash



Figure 13: Case that a task fails in an infinite loop because the critic module failed to stop the agent when its planned action is no longer suitable.

Task: Move two CDs to the bottom drawer of the desk

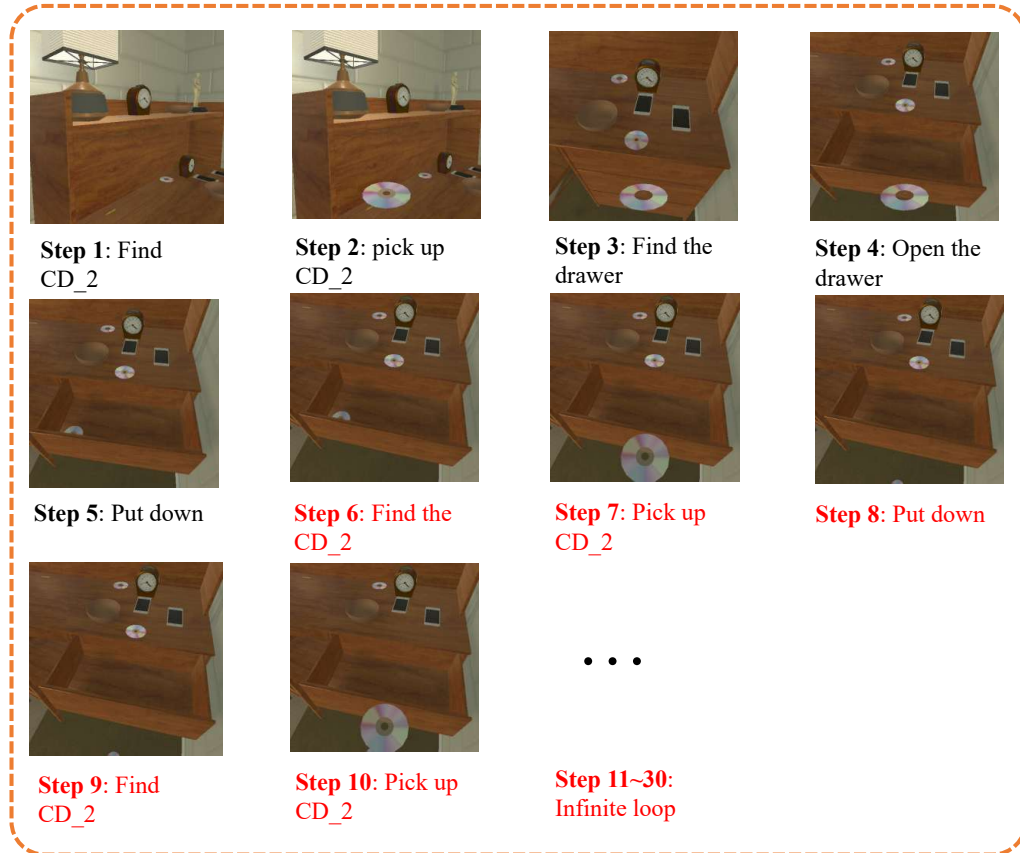


Figure 14: Case that a task fails in an infinite loop because of inaccurate action planning.